# Mode Coupling and Power Transfer in a Coaxial Sector Waveguide with a Sector Angle Taper

ARNE W. FLIFLET, LARRY R. BARNETT, MEMBER, IEEE, AND J. MARK BAIRD, MEMBER, IEEE

***Abstract*—We report a theoretical study of mode coupling and power transfer in a coaxial sector taper. The power transferred from the desired $TE_{01}$ mode into other propagating modes is calculated as a function of taper length and operating frequency. Power transfer via mode coupling involves at least three other modes: $TE_{21}$, $TE_{22}$, and $TM_{21}$. Power transfer as a function of final sector angle is also shown. At sector angles greater than 180° the taper is highly over-moded. This type of waveguide taper is utilized to feed a wide-band input coupler for gyrotron traveling wave amplifiers.**

## I. Introduction

THE DEVELOPMENT of high-power millimeter wave gyrotrons requires the availability of efficient waveguide tapers and mode couplers with high-mode selectivity. Tapers of practical interest are generally over-moded and are constrained to be compact while minimizing power conversion into spurious modes. Design criteria for tapers having circular or rectangular symmetry have been reviewed by Tang [1] but there have been few analyses of more complicated geometries. In this paper we report results from a theoretical study of mode propagation and coupling in a taper consisting of a sector of a coaxial waveguide with variable sector angle. An application of this taper is the transformation of the $TE_{10}$ mode of a rectangular waveguide into the $TE_{01}$ mode of a coaxial waveguide. This type of taper is suitable for matching a rectangular waveguide to a broad-band coaxial input coupler in a Gyro-TWT amplifier [2].

A coaxial sector taper with a linear sector angle gradient was used earlier by Marcatili who suggested that improved performance could be obtained by using a more general taper gradient profile [3]. Our interest was to determine the effectiveness of this technique for coaxial sector tapers. We have also investigated the relative efficiency of a single 360° sector angle taper compared to two 180° tapers or four 90° tapers.

Our analysis of mode coupling and reflection in the taper is an application of an analysis of coupling to spurious modes derived by Solymar [4] from the generalized telegraphist's equation for a nonuniform waveguide [5]. The mode structure and sector angle variation of mode coupling is studied for tapers intended for application to gyrotrons. Power transfer from the $TE_{01}$ coaxial sector mode into the most strongly coupled higher order modes is shown as a function of taper length and microwave frequency. For a symmetric taper, these are the $TE_{21}$, $TE_{22}$, and $TM_{21}$ coaxial sector modes. We discuss the possibility of improving taper performance by varying the taper gradient profile.

Manuscript received May 20, 1980; revised September 19, 1980. This work was supported in part by the Electron Dynamics Division, Hughes Aircraft Company under the Airforce Avionics Laboratory R&D Program, and in part by the Naval Research Laboratory under Contract N00173-79-C-0447.

The authors are with B-K Dynamics, Inc., Rockville, MD 20805.

## II. Theory

If the electromagnetic fields in a nonuniform waveguide are expanded in terms of a set of transverse modes, these modes form a system of coupled transmission lines in which the field intensities in the waveguide correspond to equivalent voltages and currents. Neglecting losses, the generalized telegraphist's equation for a system of coupled transmission lines is of the form [5]

$$-\frac{dV_i}{dz} = j\beta_i K_i I_i - \sum_P T_{pi} V_p$$
$$-\frac{dI_i}{dz} = \frac{j\beta_i}{K_i} V_i + \sum_P T_{ip} I_p \tag{1}$$

where $V_i$ and $I_i$ are the equivalent voltages and currents for the mode $i$, $\beta_i$ is the propagation coefficient, and $K_i$ is the wave impedance. The coupling of the transverse modes is characterized by the voltage and current transfer coefficients which are given by

$$T_{ip} = \int_{S(z)} \boldsymbol{e}_i \cdot \frac{\partial \boldsymbol{e}_p}{\partial z} ds \tag{2}$$

where $\boldsymbol{e}_i$ and $\boldsymbol{e}_p$ are the mode vector functions [4] and $S(z)$ is the waveguide cross section. The vector functions are orthonormal on each $S(z)$ and derivable from scalar functions which satisfy

$$\nabla_t^2 \psi_p + \gamma_p^2 \psi_p = 0 \tag{3}$$

where $\gamma_p$ is the mode eigenvalue. For TM modes (subscripts in parentheses)

$$\boldsymbol{e}_{(p)} = \nabla_t \psi_{(p)} \tag{4a}$$

$$\psi_{(p)} = 0 \text{ on } C(z). \tag{4b}$$

0018-9480/80/1200-1482$00.75 ©1980 IEEE

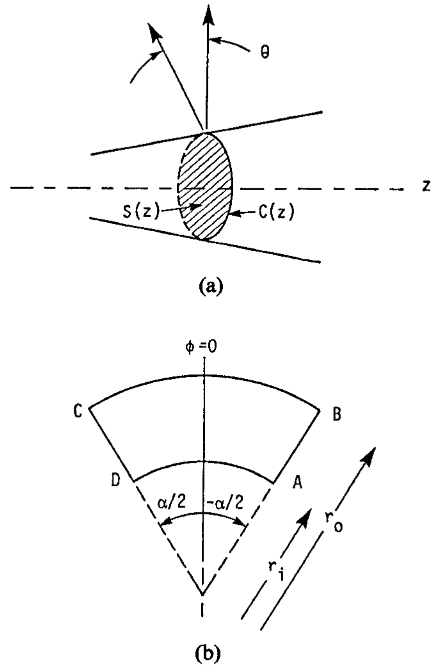


Fig. 1. (a) General view of a nonuniform waveguide. (b) Cross section of a coaxial sector waveguide.

For TE modes (subscripts in brackets)

$$e_{[p]}=\hat{z}\times\nabla\psi_{[p]} \tag{5a}$$

$$\frac{\partial\psi_{[p]}}{\partial n}=0 \text{ on } C(z) \tag{5b}$$

where $C(z)$ is the boundary of the surface $S(z)$. Expressions for the transfer coefficients in terms of line integrals over the boundary $C(z)$ have been derived by Solymar [4]. The transfer coefficient between two TE modes is given by

$$T_{[i][p]}=\frac{\gamma_{[i]}^2}{\gamma_{[p]}^2-\gamma_{[i]}^2}\int\tan\theta\,\psi_{[i]}\frac{\partial^2\psi_{[p]}}{\partial n^2}dl \tag{6a}$$

where $\theta$ is the angle between the vector normal to $C(z)$ and the vector normal to the waveguide surface as shown in Fig. 1(a). The transfer coefficient between a TE and a TM mode is given by

$$T_{[i](p)}=-\int\tan\theta\frac{\partial\psi_{[i]}}{\partial s}\frac{\partial\psi_{(p)}}{\partial n}dl \tag{6b}$$

and the transfer coefficient for reflection of a TE mode is

$$T_{[i][p]}=-1/2\int\tan\theta\left(\frac{\partial\psi_{[i]}}{\partial s}\right)^2 dl. \tag{6c}$$

In (6) the normal and tangential derivatives are indicated by $\partial/\partial n$ and $\partial/\partial s$. Consider the coaxial sector taper which is symmetric about $\phi=0$ as shown in Fig. 1(b) with sector angle $\alpha$, inner radius $r_i$, and outer radius $r_0$. In cylindical coordinates the scalar mode functions for this cross section are of the form

$$\psi_{mn}(\alpha;r,\phi)=\Phi_m(\alpha;\phi)R_m(\alpha;\gamma_{mn}r). \tag{7}$$

The angular function is of the form

$$\Phi_m(\alpha;\phi)=\left\{\begin{matrix}\sin\\ \cos\end{matrix}\right\}(\nu\phi) \tag{8}$$

where $\nu=m\pi/\alpha$ and $m=0,1,2\cdots$. The radial function is of the form

$$R_m(\alpha;\gamma_{mn}r)=a(\alpha)J_\nu(\gamma_{mn}r)+b(\alpha)Y_\nu(\gamma_{mn}r) \tag{9}$$

where $J_\nu$ and $Y_\nu$ are Bessel functions of the first and second kind of fractional order. The quantity $\gamma_{mn}a$ is the $n$th root of $R_m(\alpha;b/a\gamma_{mn}a)=0$ (TM modes) or of the derivative $R'_m=0$ (TE modes) $[b=r_0,\ a=r_i]$.

It is convenient to transform the generalized telegraphist's equation to a representation in terms of forward and backward travelling waves. Introducing as new variables the amplitudes for forward and backward travelling waves

$$A_i^+=1/2\left(K_i^{-1/2}V_i+K_i^{1/2}I_i\right) \tag{10a}$$

$$A_i^-=1/2\left(K_i^{-1/2}V_i-K_i^{1/2}I_i\right). \tag{10b}$$

Equation (1) becomes

$$\frac{dA_i^+}{dz}=-j\beta_iA_i^+-1/2\frac{d(\ln K_i)}{dz}A_i^-+\sum_p\left(S_{ip}^+A_p^++S_{ip}^-A_p^-\right)$$

$$\frac{dA_i^-}{dz}=+j\beta_iA_i^--1/2\frac{d(\ln K_i)}{dz}A_i^++\sum_p\left(S_{ip}^-A_p^++S_{ip}^+A_p^-\right) \tag{11}$$

where $S_{ip}^+$, $S_{ip}^-$ are the forward and backward coupling coefficients

$$S_{ip}^{\pm}=1/2\left[\frac{K_p^{1/2}}{K_i^{1/2}}T_{pi}\mp\frac{K_i^{1/2}}{K_p^{1/2}}T_{ip}\right]. \tag{12}$$

For tapers of practical interest the power transferred into other modes is usually small compared to the power in the main mode and we may assume that the main mode is unaffected by the presence of other modes. If we further assume that other modes are excited only the man mode $m$ and neglect coupling to evanescent modes, the amplitude of the forward travelling wave in the mode $i$ at the end of a taper of length $L$ is given by [4]

$$A_i^+(L)=\exp\left[-j\int_{z_0}^{L}\beta_i\,dz\right]\cdot\int_{z_0}^{L}S_{im}^+\exp\left[-j\int_{z_0}^{z}(\beta_m-\beta_i)\,dz'\right]dz \tag{13a}$$

where $z_0$ is the point at which the mode $i$ begins to propagate in the taper. The amplitude of the backward traveling component of the main mode due to reflection is given by

$$A_m^-(0)=-\exp\left[-j\int_0^L\beta_m\,dz\right]\int_0^L\left(S_{mm}^--1/2\frac{d(\ln K_m)}{dz}\right)\cdot\exp\left[-j2\int_0^z\beta_m\,dz'\right]dz. \tag{13b}$$

The relative power transferred into a spurious mode is

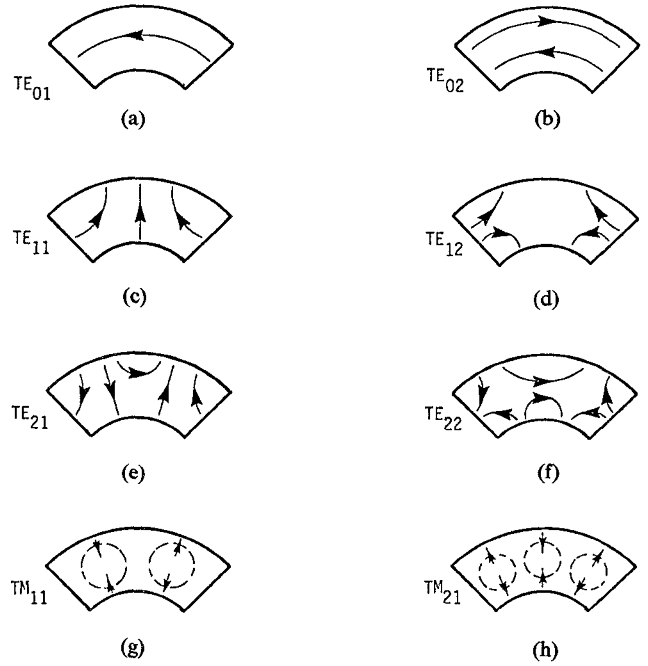


Fig. 2. Schematic cross-sectional views of low-order coaxial sector modes. Solid lines indicate $E$ fields, dashed lines indicate $H$ fields. Subscript order is $\phi, i_r$.

The relative power transferred into a spurious mode is given by

$$\frac{P_i^+}{P_m^+}=|A_i^+(L)|^2 \tag{14a}$$

for a forward traveling mode, and by

$$\frac{P_m^-}{P_m^+}=|A_m^-(0)|^2 \tag{14b}$$

for the reflection of the main mode.

## III. Calculations and Results

Schematic cross-sectional views of several low-order coaxial sector modes are shown in Fig. 2. The first mode subscript denotes the $\phi$-index and the second denotes the $r$-index. If the taper is symmetric about the $\phi=0$ plane as in Fig. 1(b), and the inner and outer radii are held constant., the $TE_{01}$ mode (Fig. 2(a)) couples only to modes with even order $\phi$-index. Thus the $TE_{01}$ mode does not couple to the modes in Fig. 2(c), 2(d), and 2(g). The coupling also vanishes between the $TE_{01}$ mode and the $TE_{02}$ shown in Fig. 2(b).

The radial components of the scalar functions satisfy the differential equation

$$\left[\frac{d^2}{dr^2}-\frac{\nu_m^2-1/4}{r^2}+\gamma_{mn}^2\right]\left(\sqrt{r}\,R_{mn}\right)=0. \tag{15}$$

This equation together with the appropriate boundary conditions constitutes an eigenvalue problem which we solve using standard finite difference techniques. The cutoff frequency of a mode is related to its eigenvalue according to

$$\omega_c=\gamma_{mn}c \tag{16}$$

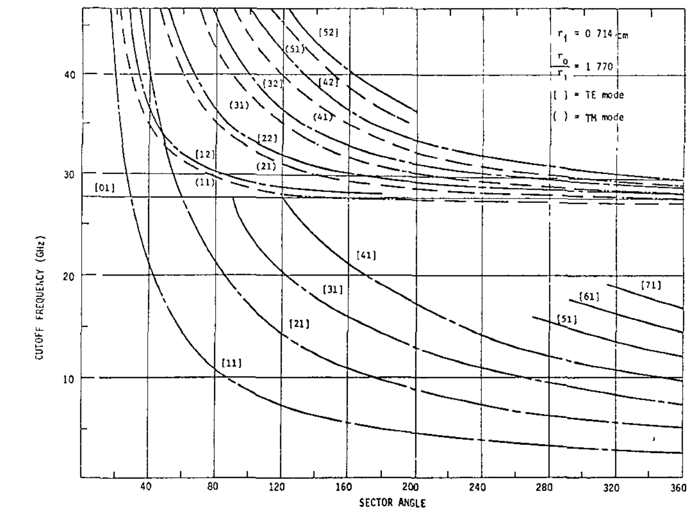


Fig. 3. Cutoff frequencies of low-lying coaxial sector modes.

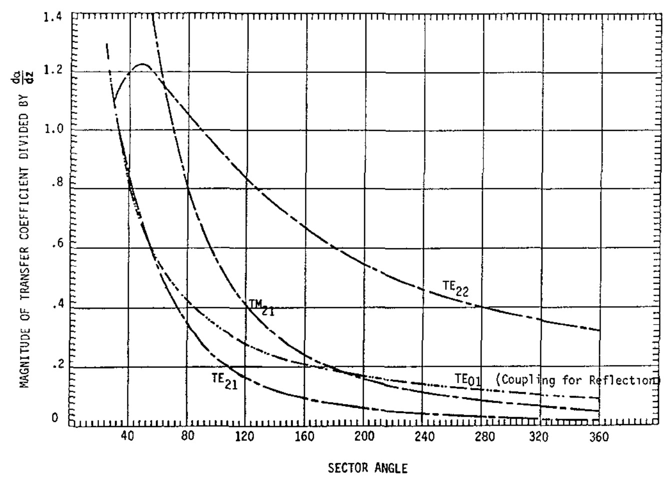


Fig. 4. Transfer coefficients for coupling of $TE_{01}$ mode to other modes.

where $c$ is the speed of light. The cutoff frequencies of several low-lying modes are shown as a function of sector angle in Fig. 3 for $r_i=0.714$ cm and $r_0=1.264$ cm. If the inner and outer radii are held constant the taper cross-sectional gradient angle $\theta$ is nonzero only along the radial line segments $AB$ and $CD$ in Fig. 1(b) and varies with radius according to

$$\tan\theta=\frac{d\alpha}{dz}r \tag{17}$$

where $d\alpha/dz$ is the sector angle gradient. It is convenient to work with the normalized transfer coefficient

$$T'=T/\frac{d\alpha}{dz}. \tag{18}$$

Normalized transfer coefficients for coupling of the $TE_{01}$ mode to the lowest even order mode are shown in Fig. 4 as a function of sector angle. Note that the wave impedence of the $TE_{01}$ mode

$$K_{[01]}=\frac{\omega\mu}{\beta_{[01]}} \tag{19}$$

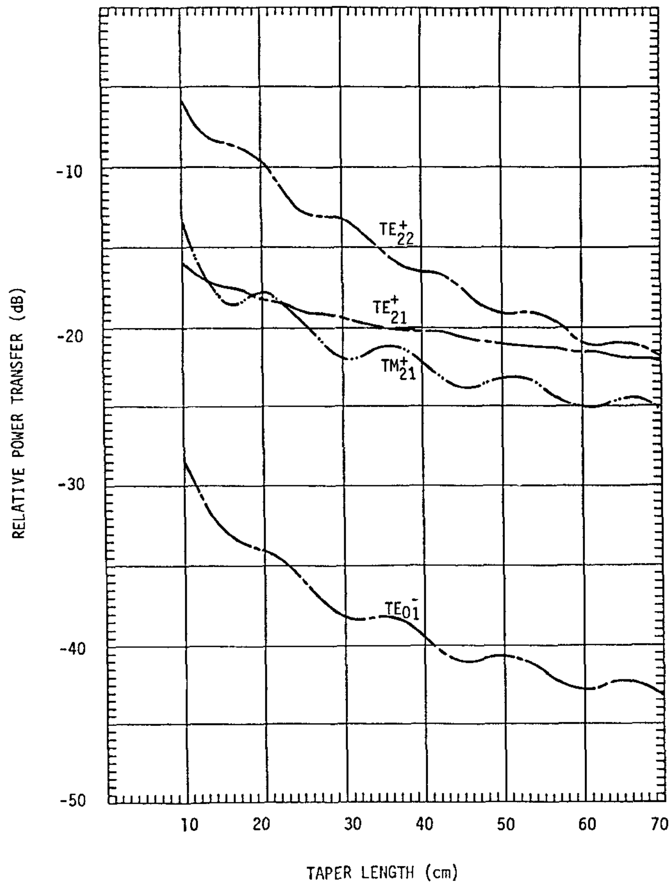


Fig. 5. Length dependence of power transfer from $TE_{01}^{+}$ mode into other modes in a linear coaxial sector taper. Frequency = 35 GHz, initial (final) sector angle = 28°(360°), $r_i$ = 0.714 cm, $r_0/r_i$ = 1.770.

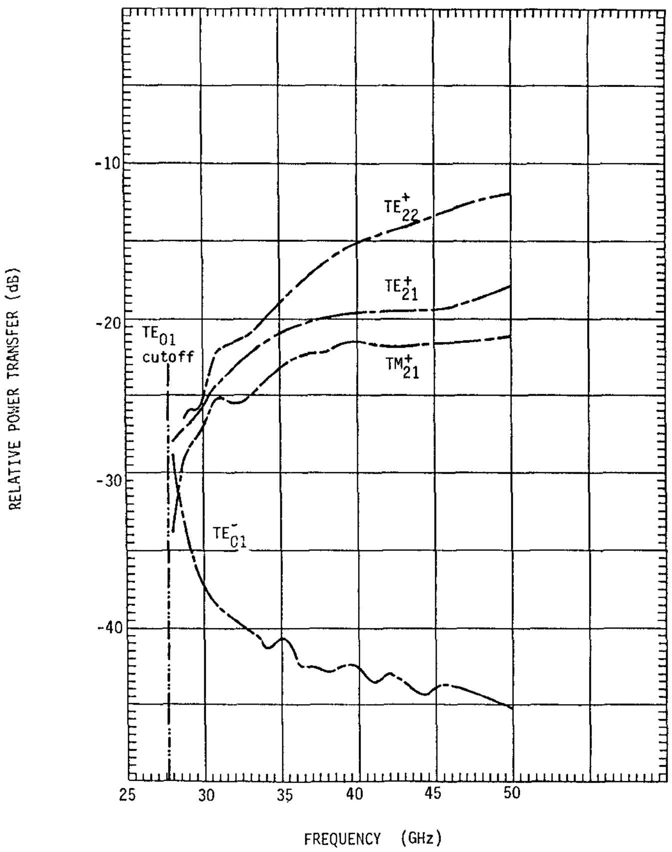


Fig. 6. Frequency dependence of power transferred from the $TE_{01}^{+}$ mode into other modes in a linear coaxial sector taper. Length = 50 cm, other dimensions are given in Fig. 5.

is independent of sector angle and, hence, $z$ so that reflection of this wave occurs only via backward coupling and not by a change in wave impedance.

Fig. 3 shows the propagating mode structure of a taper designed for a gyro-TWT amplifier operating in the region of 35 GHz. The cutoff frequency of the $TE_{01}$ mode (27.62 GHz for this taper) is independent of sector angle. As indicated in Fig. 3 only the $TE_{01}$ mode can propagate at small sector angles since the cutoff frequencies of modes with nonzero $\phi$-index vary approximately inversely with sector angle in this region. However, the taper becomes highly over-moded as the sector angle approaches 360°. The competing modes are of the form $TE_{m1}$, $TE_{m2}$, and $TM_{m1}$, $m = 1,2,3,\cdots$, although only modes with $m = 2,4,\cdots$ are coupled to the $TE_{01}$ mode in a symmetric taper. Modes with higher order $r$-index are cutoff at frequencies shown in Fig. 3.

Examination of the phase factors in (13a) and (13b) shows that power transfer between modes is likely to be important for modes with similar cutoff frequencies. Thus we may expect significant power transfer between the $TE_{01}$ and the $TE_{m2}$ and $TM_{m1}$ modes at large sector angles. On the other hand power transfer between the $TE_{01}$ and the $TE_{m1}$ modes should occur at smaller sector angles where the $TE_{m1}$ mode cutoffs intersect the $TE_{01}$ cutoff. Fig. 5 shows the relative power transfer into the $TE_{21}$, $TE_{22}$, and $TM_{21}$ forward travelling modes as a function of taper length at 35 GHz for a linear taper. The reflected power in the $TE_{01}$ backward mode, also shown in Fig. 5, is much smaller than the power transferred into forward spurious modes at this frequency. This is expected since the taper was designed with no impedance change for the $TE_{01}$ mode. Fig. 6 shows the frequency dependence of the power transfer for a linear taper of length 50 cm. The power transfer into the backward travelling $TE_{01}$ mode increases rapidly as the frequency approaches the cutoff of this mode. The results shown in Fig. 6 are probably inaccurate at low frequencies due to the neglect of power transfer into the evanescent portion of the excited modes. In addition, coupling between the $TE_{22}$ and $TM_{21}$ modes, which has been neglected, may alter the relative power transferred into these modes.

To investigate the power transfer as s function of final sector angle calculations were carried out for a 94-GHz taper design having a final sector angles of 360°, 180°, and 90°. These results are shown in Figs. 7(a), (b), and (c). This figure shows the expected decrease in power transfer into the $TE_{22}$ and $TM_{21}$ modes as the final sector angle is decreased. However, power conversion into the $TE_{21}$ mode, which couples to the $TE_{01}$ mode primarily at small

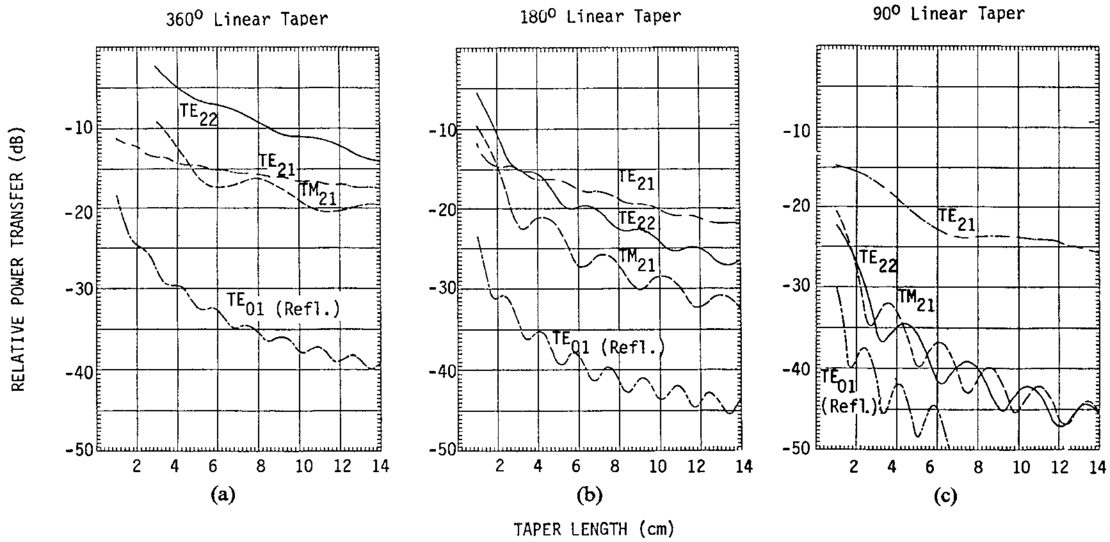


Fig. 7. Power transfer dependence on final sector angle for the $TE_{01}^{+}$ mode. Frequency = 94 GHz, $r_i = 0.2741$ cm, $r_0 = 0.5018$ cm, initial sector angle = 26.79°

sector angles, decreases less rapidly so that it becomes the dominant mode conversion process in the 90° taper.

## IV. Discussion and Conclusions

Our results indicate that the coaxial sector taper has a complicated mode structure and is highly over-moded at sector angles greater than 180°. Primary mode power loss via mode coupling involves at least three other modes: $TE_{21}$, $TE_{22}$, and $TM_{21}$. However, power loss due to mode conversion can be held within acceptable limits without impractical taper length. For example, Fig. 5 shows that power loss to mode conversion is less than $-15$ dB for a 50-cm taper operating at 35 GHz. This result assumes that the spurious modes excited in the taper are not reflected back into the taper by the microwave circuit. In this case, as pointed out by King and Marcatili [7] the taper plus reflecting circuit element may act as a high $Q$ resonator for the spurious modes leading to significant transmission loss of the primary mode at resonant frequencies. This effect can be controlled by including a dissipative filter for the spurious modes [3].

Analytical design formulas as developed previously for optimization of the taper gradient profile generally assume that coupling to only one spurious mode dominates. Our analysis shows that this simple situation does not apply to the coaxial sector taper. Moreover, it is probably difficult to improve taper performance significantly over that of a linear taper by varying the sector angle gradient. This is because the sector angle dependence of coupling of the $TE_{01}$ mode to the $TE_{21}$ mode is very different from the angular dependence of its coupling to the $TE_{22}$ and $TM_{21}$ modes.

In view of the large increase in the number of propagating modes which occurs at sector angles above 180°, the use of two 180° tapers or four 90° tapers would appear to be an effective method of reducing spurious mode generation in compact tapers provided accurate phase matching can be achieved.

## References

[1] C. C. H. Tang, "Mode conversion in nonuniform multimode waveguides and transitions," in *Advances in Microwaves*, vol. 4, L. Young Ed., New York: Academic, 1969.

[2] L. R. Barnett, J. M. Baird, and A. W. Fliflet, "Circular-electric mode waveguide couplers and junctions for use in gyrotron traveling-wave amplifier," presented at the 1980 IEEE Int. Microwave Symp., 28–30 May 1980; also, this issue; pp. 0000–0000.

[3] E. A. Marcatili, "A circular-electric hybrid junction and some channel-dropping filters," *Bell Syst. Tech. J.*, vol. 40, pp. 185–196, Jan. 1961.

[4] L. Solymar, "Spurious mode generation in nonuniform waveguide," *IRE Trans. Microwave Theory Tech.*, vol. MTT-7, pp. 379–383, July 1959.

[5] G. Reiter, "Generalized telegraphist's equation for waveguides of varying cross-sections," presented at the 1959 Convention of Long Distance Transmission by Waveguides, London, England, Jan 19–30, 1959.

[6] N. Marcuritz, *Waveguide Handbook*, vol. 10, *MIT Radiation Laboratory Series*. New York: McGraw-Hill, 1951.

[7] A. P. King, and E. A. Marcatili, "Transmission loss due to resonance of loosely coupled modes in a multi-mode system." *Bell Syst. Tech. J.*, vol. 35, pp. 899–907, July 1956.